NATIONAL ADVISORY COMMITTEE FOR AERONAUTICS

TECHNICAL NOTE 4099

HEAT TRANSFER AND BOUNDARY-LAYER TRANSITION ON TWO

BLUNT BODIES AT MACH NUMBER 3.12

By N. S. Diaconis, Richard J. Wisniewski, and John R. Jack

Lewis Flight Propulsion Laboratory
Cleveland, Ohio

NACA

Washington

October 1957

NATIONAL ADVISORY COMMITTEE FOR AERONAUTICS

TECHNICAL NOTE 4099

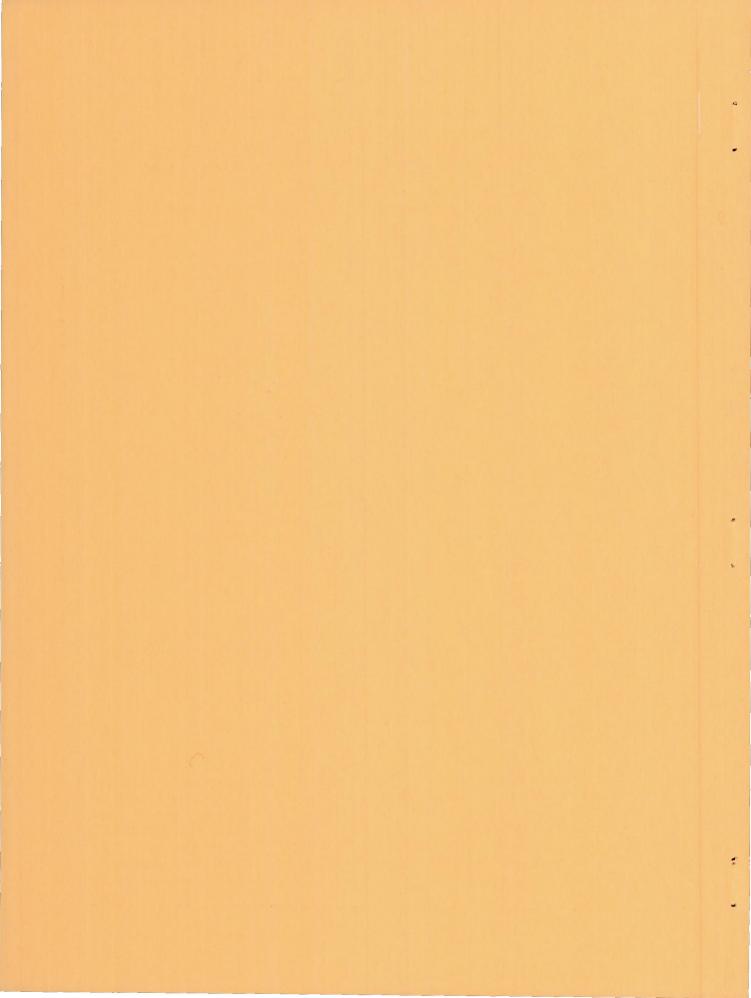HEAT TRANSFER AND BOUNDARY-LAYER TRANSITION ON TWO

BLUNT BODIES AT MACH NUMBER 3.12

By N. S. Diaconis, Richard J. Wisniewski, and John R. Jack

SUMMARY

Local heat-transfer parameters were measured on a hemisphere-cone-cylinder and on a 120°-included-angle cone-cylinder at a free-stream Mach number of 3.12 and at free-stream unit Reynolds numbers as high as 12.92×10^5 per inch. Heat-transfer data are presented for the case of wall temperature approximately equal to free-stream static temperature.

Values of the Stanton number parameter computed for both configurations (smooth surface, roughness <16 microin.) indicated good agreement with theory. When the surface roughness of the hemisphere-cone-cylinder was 130 microinches, significant increases in the local laminar-heat-transfer parameter in the hemisphere region were produced. The ratio of experimental to theoretical stagnation-point heat-transfer rate appeared to be a function of roughness Reynolds number. The ratio of local experimental heat-transfer coefficients at other points on the hemisphere to the experimental stagnation-point heat-transfer coefficient closely followed prediction by laminar theories.

Examination of the boundary-layer transition results on both bodies showed an increase in transition Reynolds number with increase in wall temperature. For a given wall temperature both surface roughness size and unit Reynolds number had a large effect on transition on the hemisphere-cone-cylinder.

INTRODUCTION

Considerations of flight at high supersonic and hypersonic velocities and the problem of high-speed atmospheric reentry have focused attention on aerodynamic heating as a major design obstacle. Extreme heating rates and low heat capacities at the tip regions of sharp-nosed bodies rule out their use at very high flight speeds. In looking for body shapes that will help to reduce the severe aerodynamic heating in the nose region, attention has been directed to the blunt body (see ref. 1) because it has

a lower heat-transfer rate than a pointed body, a larger mass (more heat capacity), and is easier to cool.

One basic configuration being tested is the hemisphere-cylinder. Laminar-heat-transfer data for hemisphere-cylinder models at Mach numbers from 2 to 8 are reported in references 2 to 6.

In order to provide further data on suitable body shapes an experimental heat-transfer and transition study was made on two blunt bodies at Mach number 3.12. Heat-transfer and transition tests were conducted on a 1.4-inch-diameter hemisphere-cone-cylinder and a 120°-included-angle cone-cylinder at ratios of wall to free-stream static-temperature as low as 0.66. On the hemisphere-cone-cylinder additional tests were performed with a roughened surface at free-stream unit Reynolds numbers as large as 12.92×10^5 per inch.

APPARATUS AND PROCEDURE

The experimental investigation was conducted in the NACA Lewis 1- by 1-foot supersonic wind tunnel at a free-stream Mach number of 3.12. Shown in figure 1 are sketches of both the hemisphere-cone-cylinder and the 120°-included-angle cone-cylinder with locations of the static-pressure taps and calibrated copper-constantan thermocouples.[1] Measured pressure distributions associated with each configuration are shown in figure 2. The thin-shell models were constructed of "K" monel. Wall thickness was determined by cutting the models open after the tests had been completed and measuring locally at each thermocouple station. Nominal thickness for the hemisphere-cone-cylinder was 1/16 inch, whereas that for the 120°-cone-cylinder was 1/25 inch.

The surface roughness of both models, on the average, was less than 16 microinches. Data were also obtained for the hemisphere-cone-cylinder when its surface was sand-blasted to approximately a 130-microinch roughness. A photograph of this finish is shown in figure 3.

The models were precooled to a wall to free-stream static-temperature ratio of 0.66, and temperature-time histories were recorded as the configurations warmed up from aerodynamic heating. Further details of the test procedure are available in reference 7. The free-stream unit Reynolds numbers of the tests on the hemisphere-cone-cylinder varied from 1.04×10^5 to 12.92×10^5 per inch. For the 120°-cone-cylinder data were obtained for unit Reynolds numbers as high as 6.67×10^5 per inch.

---

[1]The hemisphere portion of the hemisphere-cone-cylinder was initially instrumented with only half the thermocouples as shown in figure 1. Later in the program more thermocouples were added, which explains the apparent lack of data at some thermocouple positions in the subsequent figures.

Calculation of the heat transfer to the thin-skin models can be determined from the following heat-balance expression (see appendix A for symbols).

$$Q_{absorbed} = Q_{convected} + Q_{conducted} + Q_{radiated}$$

Examination of the radiation losses indicated that they would be less than 2 percent of the heat transfer by convection and consequently were neglected in the calculations. The heat transfer by conduction to the inside of these models was also negligible (see appendix B of ref. 8). Because of difficulties in construction, the wall thickness in the region of the stagnation point on both models was considerably greater than had been anticipated. To minimize the conduction losses both normal to and along the skin the data analysis was restricted to very early times in each run. (A typical surface temperature distribution can be seen in fig. 4. The axial conduction error for such a temperature distribution would be less than 5 percent.) Consequently, heat-transfer coefficients could then be computed from the following approximate relation with a minimum of error:

$$Q_{absorbed} = Q_{convected}$$

$$\rho_b c_{p,b} b \frac{dT_w}{dt} = h(T_w - T_{ad}) \tag{1}$$

where

$$T_{ad} = T_1\left(1 + \frac{\gamma - 1}{2} \eta M_1^2\right)$$

and

$$\eta = \begin{cases} \sqrt{Pr} \text{ laminar} \\ \sqrt[3]{Pr} \text{ turbulent} \end{cases}$$

Stanton numbers based on free-stream properties were then determined from the expression

$$St_0 = \frac{h}{\rho_0 u_0 c_{p,0}} \tag{2}$$

Details of the calculation procedure are similar to those described in reference 8 for the cone-cylinder and parabolic-nosed-cylinder bodies. The accuracy of the various parameters in the computations can also be found in reference 8. (Stanton numbers computed from the present results

could have a maximum error of ±18 percent if all the errors were addi-
tive; however, it is believed that the data are considerably more accu-
rate than this value.) The condensation films that were observed in the
tests discussed in reference 8 were also present in this series of ex-
periments. As in the previous case, it is believed that these films had
negligible effects on the final results.

RESULTS AND DISCUSSION

Heat Transfer without Roughness

Local heat-transfer data are presented for the hemisphere-cone-
cylinder model in figure 5(a) where the parameter $St_0 \sqrt{\dfrac{u_0 d}{\nu_0}}$ is plotted
against dimensionless surface distance. Even though the free-stream
unit Reynolds number $\dfrac{u_0}{\nu_0}$ was varied over a large range (1.04×10^5 to
12.92×10^5 per in.) there does not appear to be any dependence on $\dfrac{u_0}{\nu_0}$ in
the laminar region. Also shown in the figure is the theoretical vari-
ation of the laminar-heat-transfer coefficient given by Reshotko in ref-
erence 9. Stanton number for an isothermal surface according to refer-
ence 9 can be expressed as

$$St_0 \sqrt{\frac{u_0 d}{\nu_0}} = \frac{2l}{\left(\dfrac{C_f Re_w}{Nu}\right)} Pr_w^{\alpha - 1} \sqrt{\frac{\left(\dfrac{p_1}{p_0}\right)\left(\dfrac{u_1}{u_0}\right)\left(\dfrac{\mu_w}{\mu_0}\right)\left(\dfrac{T_0}{T_w}\right)}{\dfrac{\Theta}{d}}} \tag{3}$$

where

$$\frac{\Theta}{d} = \frac{A}{\left(\dfrac{T_1}{T_t}\right)^K M_1^{B-1} r^2} \int_0^{x/d} r^2 \left(\frac{T_1}{T_t}\right)^K M_1^{B-1} \, d\!\left(\frac{x}{d}\right)$$

$$A = 0.44$$

$$\frac{l}{\left(\dfrac{C_f Re_w}{Nu}\right)} = 0.10$$

$$K = 4 \quad \text{for} \quad \gamma = 1.4$$

and

$\alpha = 1/2$ for large favorable pressure gradients (hemisphere) and 1/3 for small pressure gradients (cone-cylinder)

Since an isothermal temperature level must be chosen for the above, free-stream static temperature was selected (B = 3.50 from fig. 1 of ref. 9) as this temperature level was closest to model surface conditions at the 5-second test time. The Prandtl number for this wall temperature is 0.77.

At the stagnation point the heat-transfer parameter can be evaluated by making certain simplifying assumptions. If the Mach number M_1, the velocity u_1, and the local radius r are assumed linear in the vicinity of the stagnation point, the expression for $St_0 \sqrt{u_0 d / \nu_0}$ becomes independent of x, but is a function of the local Mach number gradient. This gradient was evaluated by fitting the experimental Mach number data with a straight line between the stagnation point and the sonic point on the body. Such a fairing very closely approximates the experimental Mach number distribution on the forward portion of the hemisphere. The calculated stagnation value of $St_0 \sqrt{\dfrac{u_0 d}{\nu_0}}$ then becomes 3.44. Figure 5(a) shows that the agreement with the isothermal theory is adequate, especially on the forward portion of the hemisphere. Downstream on the cone and the cylinder there are large deviations from the laminar theory, but this is attributed to transition to turbulent flow.

The next largest deviations from theory occur on the aft portion of the hemisphere. To determine whether axial temperature gradients could account for these discrepancies, the modified method of Lighthill (ref. 10) was applied to axisymmetric stagnation-point flow (see appendix B). The results indicate an increase in the computed value of $St_0 \sqrt{\dfrac{u_0 d}{\nu_0}}$ of only 5 percent on the aft portion of the hemisphere. At the stagnation point, theory indicates no change from the isothermal value. Previous investigations on slender bodies of revolution (ref. 8) indicated a large influence of temperature gradient. However, in the calculations of reference 8 the leading edge was assumed to be at the adiabatic wall temperature. The temperature gradient that existed over the hemisphere in the present tests was much less severe and apparently did not affect the results as much.

The experimental results for the 120°-cone-cylinder are shown in figure 5(b). Data are presented for three values of unit Reynolds number and, as for the hemisphere-cone-cylinder, no appreciable effect of u_0 / ν_0

is indicated on the laminar heat transfer. Comparison is also made with the theory of Reshotko (ref. 9), and good agreement is indicated. Results at the stagnation point shown in the inset also indicate satisfactory agreement with theory; however this agreement may be open to question. The calculated stagnation-point heat-transfer rate is directly proportional to the square root of the Mach number gradient. For these calculations, a linear Mach number variation based on the measured pressure coefficients of figure 2(b) was used. Since the fairing of the pressure-coefficient curve is somewhat arbitrary, the calculated value of Stanton number must also be considered arbitrary within certain limits. Note that this discussion applies only at the stagnation point; the theoretical curve downstream of the stagnation point is not affected by this fairing.

Heat Transfer with Distributed Roughness

Calculated values of the heat-transfer parameter $St_0 \sqrt{\dfrac{u_0 d}{\nu_0}}$

for the hemisphere-cone-cylinder, sand-blasted to a surface roughness of 130 microinches, are shown in figure 6. The data for the hemisphere show a definite increase in heat-transfer parameter with an increase in the unit Reynolds number beyond 5.62×10^5 per inch. The form of the decrease of the data with increase in x indicates that these results represent laminar flow and not turbulent flow. Had the boundary layer been turbulent, a variation as depicted by the dotted curve (Van Driest, ref. 11 for $u_0 / \nu_0 = 12.92 \times 10^5$ per in.) would have been expected. This is clearly not obtained. As further evidence for laminar flow these results and one set of data for the smooth configuration are plotted in figure 7 as the ratio of local to stagnation heat-transfer rate. The agreement in trend with the laminar theories of both references 9 and 12 and with the smooth model results indicates that the flow over the roughened hemisphere is laminar. It is obvious that the data do not agree with the theoretical ratio of turbulent to laminar stagnation-point heat transfer. This agreement with laminar theory suggests a means of correlating the experimental stagnation-point heating rate in terms of roughness Reynolds number $\dfrac{u_0 H}{\nu_0}$. Such a correlation together with the local heating-rate distribution of, for example, Lees (ref. 12) could be applied to predict laminar-heat-transfer coefficients over the entire hemisphere.

Figure 8 is a plot of the ratio of experimental to theoretical stagnation-point heating rates as a function of roughness Reynolds number Re_H. As Re_H increases, the effect of roughness becomes more pronounced. The data also show that a critical value of roughness Reynolds number may

exist for these tests above which roughness begins to affect the heat transfer. However, because of the scarcity of data and the limited test conditions, it is not proposed that these results would be applicable universally to laminar flows over roughened blunt bodies.

At present there is no explanation of the increase in the laminar heating rate due to roughness. In fact, there are indications that this effect may not occur on all configurations at the same free-stream conditions. Unpublished NACA data on a $9\frac{1}{2}°$ -included-angle cone-cylinder, hemispherically blunted to a $\frac{3}{16}$-inch tip diameter, show no increase in the laminar Stanton number on either the conical or cylindrical portions with roughness as large as 500 microinches. The present limited results indicate, therefore, that the effect of roughness near the nose of a very blunt body is more pronounced than it is on a slender body.

Boundary-Layer Transition

Figure 9 shows for the hemisphere-cone-cylinder values of the parameter $St_0\sqrt{\frac{u_0 d}{\nu_0}}$ for two temperature ratios at a free-stream unit Reynolds number per inch of 6.67×10^5. Transition to turbulent flow on the body is indicated by the abrupt increase in the local heat-transfer parameter. Examination of the two sets of data, in figure 9, reveals the boundary layer to be entirely laminar at the higher temperature ratio, whereas transition is located on the body at the lower temperature ratio. This interesting behavior is contrary to that expected from stability theory and is referred to as transition reversal. The transition reversal phenomenon, which has been observed on slender shapes as well as on the present blunt shapes, is discussed more fully in reference 13.

The effect of surface cooling on transition on the hemisphere-cone-cylinder is summarized in figure 10(a) for unit Reynolds numbers ranging from 5.62×10^5 to 12.92×10^5 per inch. For this plot, the sudden increase in the time rate of change of temperature (which is also associated with the abrupt increase in the local heat-transfer coefficient) was chosen as the start of transition (ref. 7). Here, it is evident that heating the model increases the transition Reynolds number ($Re_{x,tr} = u_0 x_{tr}/\nu_0$) until the transition point moves off the model. Continued heating to the adiabatic temperature does not cause the transition point to reappear. In addition, figure 10(a) illustrates that an increase in the unit Reynolds number at a given temperature ratio decreased the transition Reynolds number. This observed variation with unit Reynolds number in this temperature range is contrary to that normally obtained at adiabatic wall conditions.

Transition data were also obtained with a surface roughness of 130 microinches. These data are presented in figure 10(b) for two unit Reynolds numbers. For comparison, data are also included for a surface roughness of 16 microinches at a unit Reynolds number of 6.67×10^5 per inch. Inspection of figure 10(b) shows that increasing the roughness by a factor of about 10 reduces the transition Reynolds number to between one-half and one-fourth of the smooth-surface value for temperature ratios around 1.2. Furthermore, increasing the unit Reynolds number also reduces the transition Reynolds number.

Finally, figure 11 shows the transition results obtained on the 120°-cone-cylinder. Unlike the hemisphere-cone-cylinder this configuration displays the complete cycle of boundary-layer transition. The data for the highest Reynolds number per inch indicate that the transition-point movement is completely contained on the model for the entire temperature range. (The last thermocouple on the body at this value of u_0/ν_0 always indicated a turbulent heat-transfer rate.) At lower values of u_0/ν_0 the transition point is on the body at the low temperatures, moves off at intermediate temperatures, and comes back on the body as the adiabatic temperature is approached. A more detailed discussion of this phenomenon is given in reference 13.

SUMMARY OF RESULTS

Local heat-transfer rates were measured on a hemisphere-cone-cylinder and on a 120°-cone-cylinder at a Mach number of 3.12 and free-stream unit Reynolds numbers as large as 12.92×10^5 and 6.67×10^5 per inch, respectively. Results are presented for the conditions of model surface temperature approximately equal to free-stream static temperature.

Experimental values of the heat-transfer parameter $St_0 \sqrt{\dfrac{u_0 d}{\nu_0}}$ showed good agreement on both bodies with predictions by theory when the surface roughness was less than 16 microinches. However, the calculations indicated that a reliable prediction of the heat transfer near the stagnation point on the 120°-cone-cylinder would require accurate knowledge of the local Mach number gradient in that region.

Sand-blasting the hemisphere-cone-cylinder body to a surface roughness of 130 microinches produced appreciable increases in the local laminar-heat-transfer parameter over the hemisphere. It was found that the ratio of experimental to theoretical stagnation-point heat-transfer rate could be correlated for these tests on the basis of a roughness Reynolds number Re_H. The heat transfer at other locations on the hemisphere could be predicted by theory in conjunction with the stagnation-point correlation.

The behavior of boundary-layer transition on both bodies was also examined. Results showed that, contrary to expected trends based on stability theory, increasing the wall temperature increased the transition Reynolds number. This trend was obtained on the hemisphere-cone-cylinder with both rough and smooth surfaces. For a given surface temperature on that body both surface roughness size and unit Reynolds number had large effects on the transition Reynolds number. On the 120°-cone-cylinder only tests with a smooth surface were performed. Results were similar to those on the smooth hemisphere-cone-cylinder.

Lewis Flight Propulsion Laboratory
    National Advisory Committee for Aeronautics
        Cleveland, Ohio, August 15, 1957

APPENDIX A

SYMBOLS

A, B, K, α constants in eq. (3)

b   skin thickness

C_f local skin-friction coefficient

C_p pressure coefficient

c_p specific heat at constant pressure

D   constant defined by eq. (B5)

d   characteristic length: (a) hemisphere diameter for hemisphere-cone-cylinder, (b) maximum body diameter for 120°-cone-cylinder

E   constant defined by eq. (B7)

F   constant defined by eq. (B10)

$f''(0)$ Blasius wall shear function

g   constant in expression $T_{ref} - T_w(x) = gx^\beta$

H   surface roughness height

h   local heat-transfer coefficient

$\bar{h}$ local heat-transfer coefficient for isothermal wall

k   thermal conductivity

l dimensionless shear parameter (ref. 9)

$\left(\dfrac{l}{\frac{C_f Re_w}{Nu}}\right)$ heat-transfer parameter (ref. 9)

M   Mach number

m   constant defined by eq. (B3)

Nu   Nusselt number

Pr   Prandtl number

p   pressure

Q   total heat flow

q   heat-transfer rate

Re_H roughness Reynolds number, $\dfrac{u_0}{\nu_0} H$

Re_x length Reynolds number, $\dfrac{u_0}{\nu_0} x$

r   local radius of model

St   Stanton number

T   temperature

T_t stagnation temperature, $^{\circ}R$

t   time

u   velocity

x   surface distance

z   parameter defined by eq. (B1)

β exponent defined by expression $T_{ref} - T_w(x) = gx^{\beta}$

$\Gamma()$ gamma function

γ ratio of specific heats

η recovery factor

Θ $\dfrac{A}{\left(\dfrac{T_1}{T_t}\right)^K M_1^{B-1} r^2} \displaystyle\int_0^x r^2 \left(\dfrac{T_1}{T_t}\right)^K M_1^{B-1}\, dx$

θ angular displacement

μ viscosity coefficient

ν kinematic viscosity

ξ parameter defined by eq. (B8)

ρ density

τ shear stress

Subscripts:

ad   adiabatic wall

av   average

b   model

max   maximum

ref   reference condition

s   stagnation point

th   theoretical

tr   transition

w   model wall

0   free stream ahead of shock wave

1   edge of boundary layer

APPENDIX B

STAGNATION-POINT HEAT-TRANSFER COEFFICIENT FOR VARIABLE

WALL TEMPERATURE

Reshotko and Cohen, in reference 14, point out that exact methods such as Lighthill's for predicting nonisothermal heat-transfer coefficient do not apply near a stagnation point because of the omission of the term $\frac{\partial}{\partial x}\left(k\,\frac{\partial T}{\partial x}\right)$ in the energy equation. However, it can be shown that this term can be dropped from the equation if the surface temperature distribution is expressed as $T_{ref} - T_w(x) = gx^{\beta}$, where the exponent β assumes values of 2 or greater.

According to Tifford (ref. 10), Lighthill's expression for a two-dimensional model surface with zero pressure gradient may be written as follows for compressible flow:

$$q(x) = -0.538\ k_1\left(\frac{Pr\rho_1}{\mu_1^2}\right)^{1/3}\sqrt{\tau(x)}\left\{(T_w - T_{ad})_{x=0}\left[\int_0^x \sqrt{\tau(x)}\ dx\right]^{-1/3} + \right.$$

$$\left. \int_0^x\left[\int_z^x \sqrt{\tau(x)}\ dx\right]^{-1/3}\left[\frac{d(T_w - T_{ad})}{dz}\right]dz\right\} \tag{B1}$$

where

$$\tau(x) = \mu_1\left(\frac{\partial u}{\partial y}\right)_{y=0} = \mu_1 u_1 f''(0)\sqrt{\frac{u_1}{\nu_1 x}} \tag{B2}$$

For supersonic flow in the region of the stagnation point on a closed body of revolution (e.g., a sphere), the velocity at the edge of the boundary layer may be written

$$u_1 = mx \tag{B3}$$

When this velocity field is operated on by Mangler's transformation, the result is a flow field that can be represented very closely by the expression

$$u_1 = mx^{1/3} \tag{B4}$$

Substituting this into equation (B2) then gives

$$\tau(x) = \mu_1 f''(0) m^{3/2} \nu_1^{-1/2} = \text{constant} = D \tag{B5}$$

With this expression for the shear stress, the local heating rate is

$$q(x) = E\left[\frac{(T_w - T_{ad})_{x=0}}{x^{1/3}} + \int_0^x \frac{\dfrac{d(T_w - T_{ad})}{dz}}{(x - z)^{1/3}}\, dz\right] \tag{B6}$$

where

$$E = -\frac{k_1}{(1/3)!}\left(\frac{\mathrm{Pr}\rho_1}{9\mu_1^2}\right)^{1/3} D^{1/3} \tag{B7}$$

Letting

$$z = x\xi \tag{B8}$$

equation (B6) then becomes

$$q(x) = \frac{E}{x^{1/3}}\left[(T_w - T_{ad})_{x=0} + \int_0^1 \frac{\dfrac{d(T_w - T_{ad})}{d\xi}}{(1 - \xi)^{1/3}}\, d\xi\right] \tag{B9}$$

If the surface temperature distribution is represented as

$$T_w(z) - T_{ad}(z) = \left[T_w(0) - T_{ad}(0)\right] + Fz^\beta = T_w(0) - T_{ad}(0) + F(x\xi)^\beta$$
$$\tag{B10}$$

and substituted into equation (B9), the local heat-transfer rate then becomes

$$q(x) = \frac{E}{x^{1/3}}\left[(T_w - T_{ad})_{x=0} + F\beta x^\beta \frac{\Gamma(\beta)\Gamma(2/3)}{\Gamma(\beta + 2/3)}\right] \tag{B11}$$

Now since

$$Fx^\beta = T_w(x) - T_{ad}(x) - \left[T_w(0) - T_{ad}(0)\right]$$

and

$$\frac{E}{x^{1/3}} = \frac{-\left[f''(0)\right]^{1/3}}{(1/3)!(9)^{1/3}}\, \mathrm{Pr}^{1/3}\frac{k_1}{x}\sqrt{\mathrm{Re}} = -0.592\, \mathrm{Pr}^{1/3}\frac{k_1}{x}\sqrt{\mathrm{Re}} = \bar{h}$$

then   then

$$q(x) = \bar{h}\left(\Big[T_w(0) - T_{ad}(0)\Big] + \beta\Big\{T_w(x) - T_{ad}(x) - \Big[T_w(0) - T_{ad}(0)\Big]\Big\}\right.$$
$$\left.\frac{\Gamma(\beta)\Gamma(2/3)}{\Gamma(\beta + 2/3)}\right)$$ (B12)

Since

$$q(x) = h\Big[T_w(x) - T_{ad}(x)\Big]$$

$$\frac{h}{\bar{h}} = \frac{T_w(0) - T_{ad}(0)}{T_w(x) - T_{ad}(x)} + \beta\left[1 - \frac{T_w(0) - T_{ad}(0)}{T_w(x) - T_{ad}(x)}\right]\frac{\Gamma(\beta)\Gamma(2/3)}{\Gamma(\beta + 2/3)}$$ (B13)
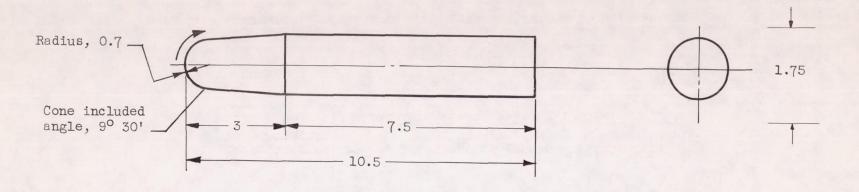
REFERENCES

1. Allen, H. Julian, and Eggers, A. J., Jr.: A Study of the Motion and Aerodynamic Heating of Missiles Entering the Earth's Atmosphere at High Supersonic Speeds. NACA RM A53D28, 1953.

2. Korobkin, I.: Laminar Heat Transfer Characteristics of a Hemisphere for the Mach Number Range 1.9 to 4.9. NAVORD Rep. 3841, U.S. Naval Ord. Lab., Oct. 10, 1954.

3. Stine, Howard A., and Wanlass, Kent: Theoretical and Experimental Investigation of Aerodynamic-Heating and Isothermal Heat-Transfer Parameters on a Hemispherical Nose with Laminar Boundary Layer at Supersonic Mach Numbers. NACA TN 3344, 1954.

4. Winkler, E. M., and Danberg, J. E.: Heat Transfer Characteristics of a Hemisphere Cylinder at Hypersonic Mach Numbers. Preprint No. 622, Inst. Aero. Sci., 1956.

5. Gruenwald, K. H., and Fleming, W. J.: Laminar Heat Transfer to a Hemisphere at Mach Number 3.2 and at Low Heat-Transfer Rates. NAVORD Rep. 3980, U.S. Naval Ord. Lab., Feb. 20, 1956.

6. Crawford, Davis H., and McCauley, William D.: Investigation of the Laminar Aerodynamic Heat-Transfer Characteristics of a Hemisphere-Cylinder in the Langley 11-Inch Hypersonic Tunnel at a Mach Number of 6.8. NACA TN 3706, 1956.

7. Jack, John R., and Diaconis, N. S.: Variation of Boundary-Layer Transition with Heat Transfer on Two Bodies of Revolution at a Mach Number of 3.12. NACA TN 3562, 1955.

8. Jack, John R., and Diaconis, N. S.: Heat-Transfer Measurements on
   Two Bodies of Revolution at a Mach Number of 3.12. NACA TN 3776,
   1956.

9. Reshotko, Eli: Simplified Method for Estimating Compressible Laminar
   Heat Transfer with Pressure Gradient. NACA TN 3888, 1956.

10. Tifford, A. N.: Heat Transfer and Frictional Effects in Laminar
    Boundary Layers. Pt. 5 - The Modified Lighthill Method for Deter-
    mining the Rate of Heat Transfer. WADC TR 53-288, The Ohio State
    Univ. Res. Foundation, Nov. 1954.

11. Van Driest, E. R.: The Problem of Aerodynamic Heating. Aero. Eng.
    Rev., vol. 15, no. 10, Oct. 1956, pp. 26-41.

12. Lees, L.: Laminar Heat Transfer Over Blunt-Nosed Bodies at Hyper-
    sonic Flight Speeds. Jet Prop., vol. 26, no. 4, Apr. 1956, pp. 259-
    269; 274.

13. Jack, John R., Wisniewski, Richard J., and Diaconis, N. S.: The Ef-
    fects of Extreme Surface Cooling on Boundary-Layer Transition.
    NACA TN 4094, 1957.

14. Reshotko, Eli, and Cohen, Clarence B.: Heat Transfer at the Forward
    Stagnation Point of Blunt Bodies. NACA TN 3513, 1955.

Radius, 0.7

Cone included
angle, 9° 30'

3

7.5

10.5

1.75

Thermocouple locations at generator distance x																		
0	.12	.23	.34	.45	.56	.67	.77	.88	1.06	1.44	1.94	2.94	3.55	4.43	5.43	6.55	7.67	8.92
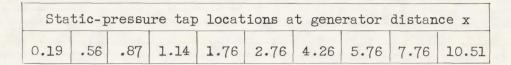
Static-pressure tap locations at generator distance x															
0.22	.45	.66	.88	1.01	1.39	1.89	2.38	2.90	3.21	3.52	4.39	5.40	6.52	7.65	8.89

CD-5782

(a) Hemisphere-cone-cylinder.

Figure 1. - Details of model and instrumentation locations. Dimensions in inches.

Total apex angle, 120°

1.75

12

Thermocouple locations at generator distance x														
0	.19	.44	.69	.94	1.26	1.76	2.76	3.76	4.76	5.76	6.76	7.76	9.01	10.51

Static-pressure tap locations at generator distance x									
0.19	.56	.87	1.14	1.76	2.76	4.26	5.76	7.76	10.51

/CD-5782/

(b) 120°-Cone-cylinder.

Figure 1. - Concluded. Details of model and instrumentation locations. Dimensions in inches.

(a) Hemisphere-cone-cylinder.
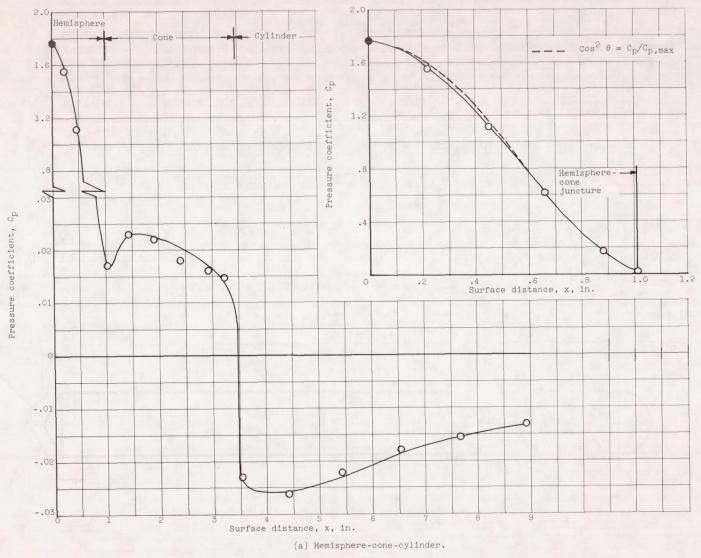
Figure 2. - Pressure distribution. Pressure coefficient at surface distance 0 is theoretical stagnation-point value.

(b) 120°-Cone-cylinder.
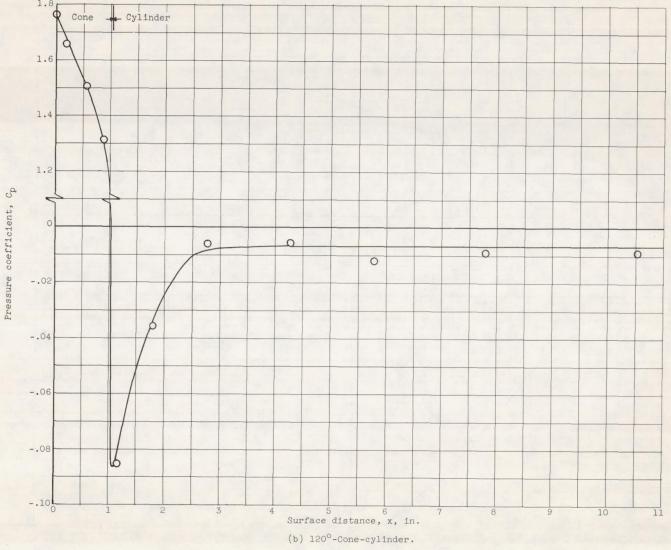
Figure 2. - Concluded. Pressure distribution. Pressure coefficient at surface distance 0 is theoretical
stagnation-point value.

4479

C-42152
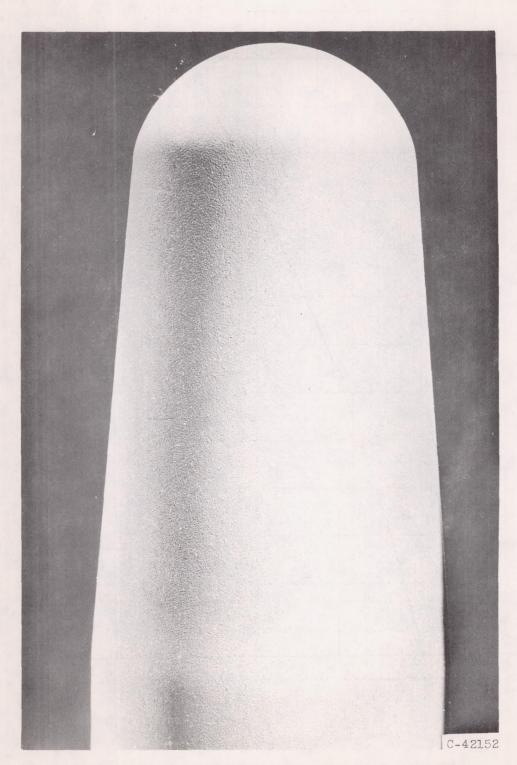
Figure 3. - Photograph of sand-blasted hemisphere-cone-cylinder. Roughness, 130 microinches.
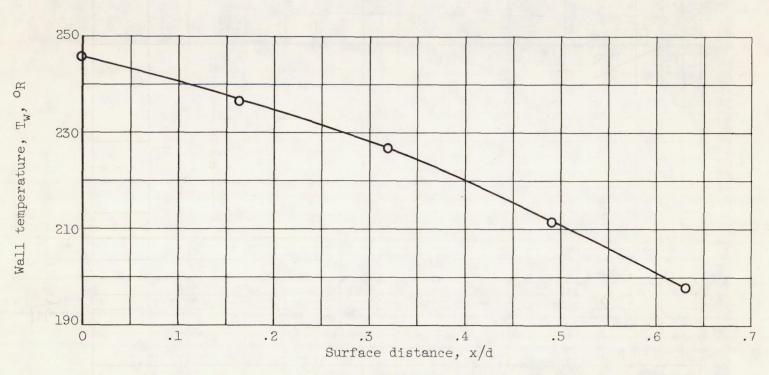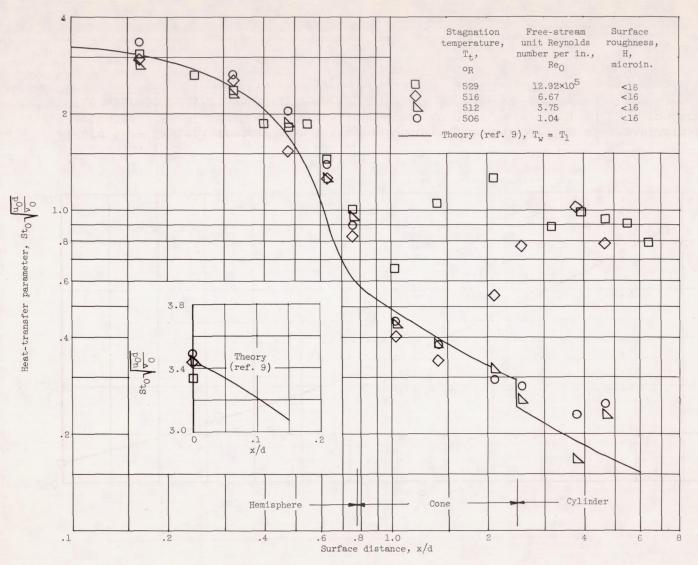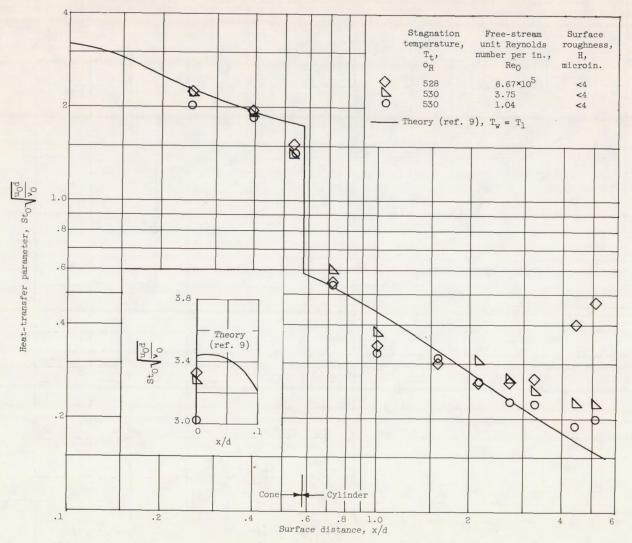
Figure 4. - Typical temperature distribution over forward portion of hemisphere-cone-cylinder. Free-stream unit Reynolds number per inch, 6.67×10^5; surface roughness, <16 microinches; stagnation temperature, 516° R; time, 5 seconds.

Stagnation temperature, T_t, °R | Free-stream unit Reynolds number per in., Re_0 | Surface roughness, H, microin.

□	529	12.92×10^5	<16
◇	516	6.67	<16
△	512	3.75	<16
○	506	1.04	<16

—— Theory (ref. 9), $T_w = T_1$

Hemisphere ——→|←—— Cone ——→|←— Cylinder

(a) Hemisphere-cone-cylinder with smooth surface.

Figure 5. - Local heat-transfer parameter.

(b) 120°-Cone-cylinder with smooth surface.

Figure 5. - Concluded. Local heat-transfer parameter.
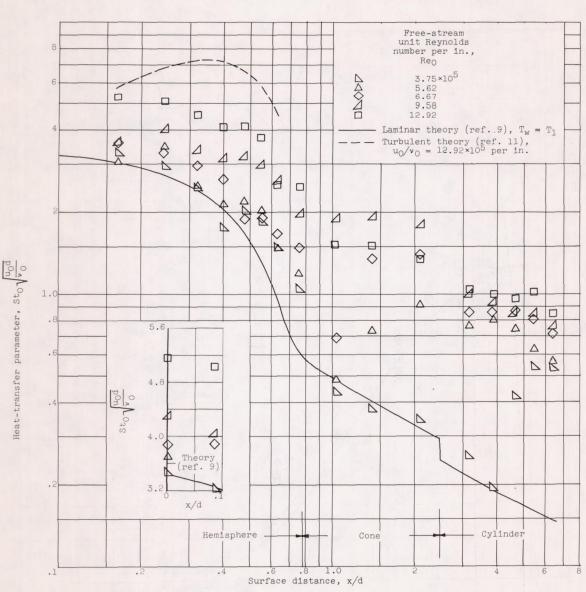
Figure 6. - Effect of roughness on heat transfer. Surface roughness, 130 microinches; stagnation temperature, 530° R.
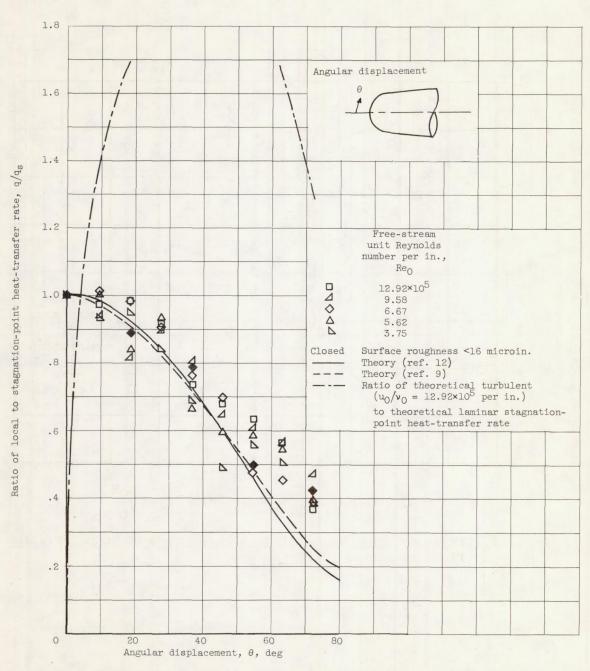
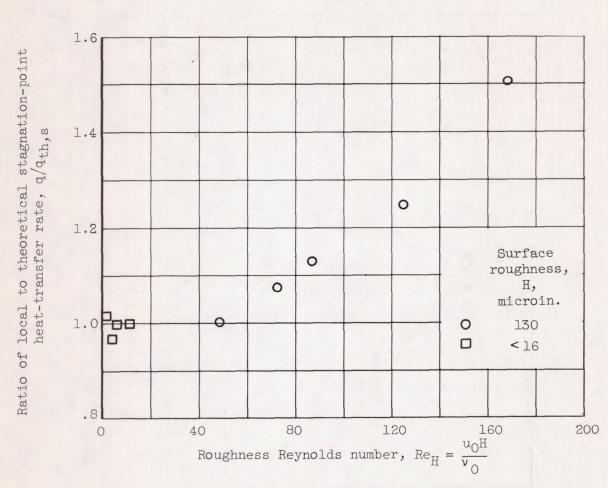Figure 7. - Laminar-heat-transfer rate on hemisphere with surface roughness of 130 microinches.

CR-4 back

4479

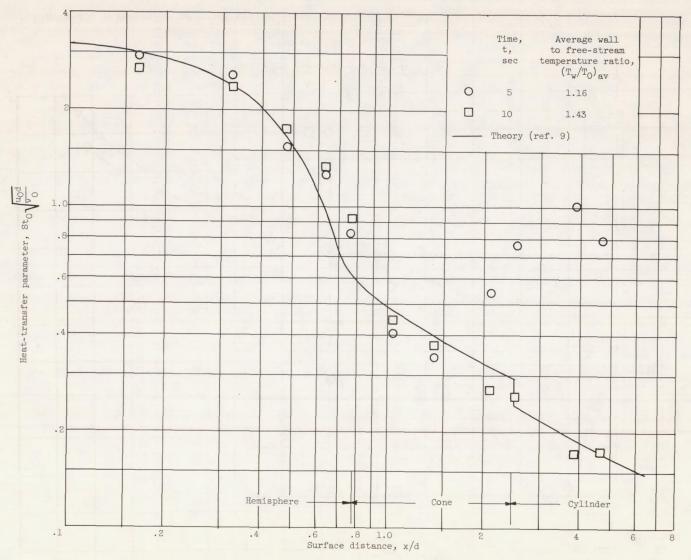Figure 8. - Variation of stagnation-point heat transfer with surface roughness parameter.

Figure 9. - Effect of extreme cooling on boundary-layer transition for hemisphere-cone-cylinder. Stagnation temperature, 516° R; free-stream unit Reynolds number per inch, 6.67×10⁵.

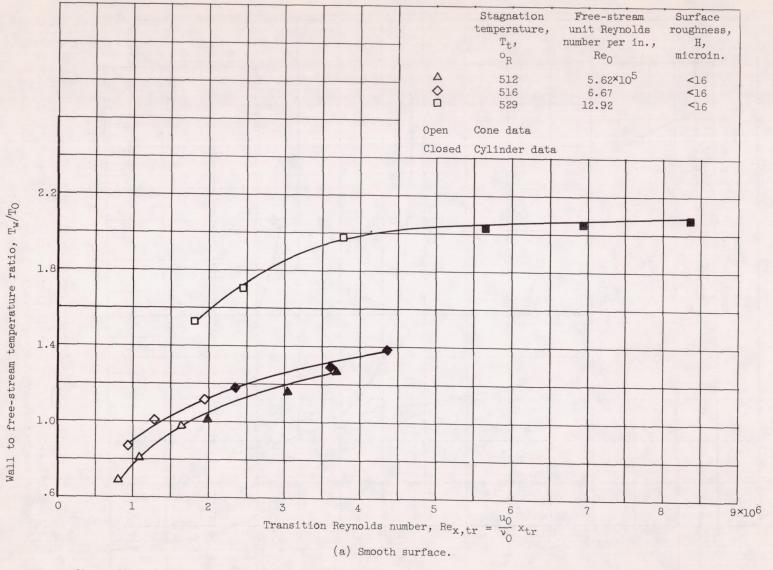|	Stagnation temperature, T_t, $^\circ R$	Free-stream unit Reynolds number per in., Re_0	Surface roughness, H, microin.
△	512	5.62×10^5	<16
◇	516	6.67	<16
□	529	12.92	<16

Open   Cone data

Closed Cylinder data

Wall to free-stream temperature ratio, T_w/T_0

2.2

1.8

1.4

1.0

.6

0   1   2   3   4   5   6   7   8 9×10^6

Transition Reynolds number, $Re_{x,tr} = \dfrac{u_0}{\nu_0} x_{tr}$

(a) Smooth surface.

Figure 10. - Variation of transition reversal with unit Reynolds number for hemisphere-cone-cylinder.

(b) Rough surface.
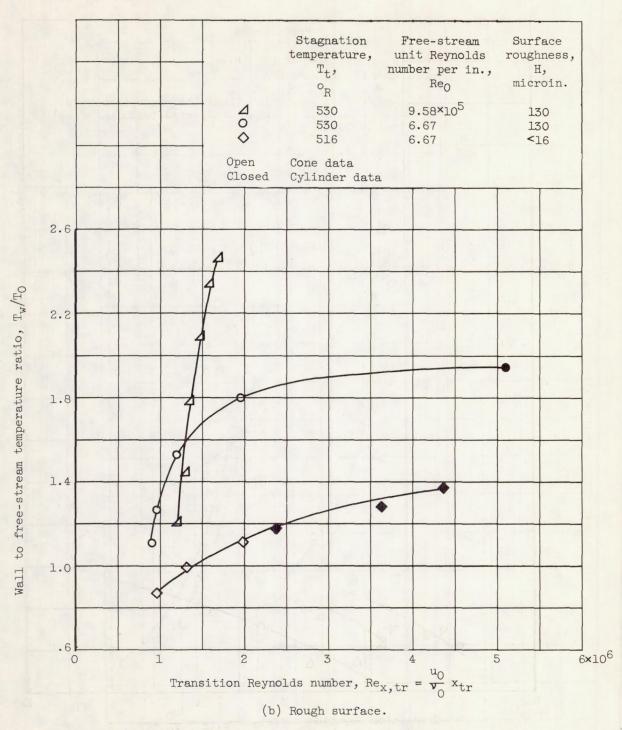
Figure 10. - Concluded. Variation of transition reversal with unit Reynolds
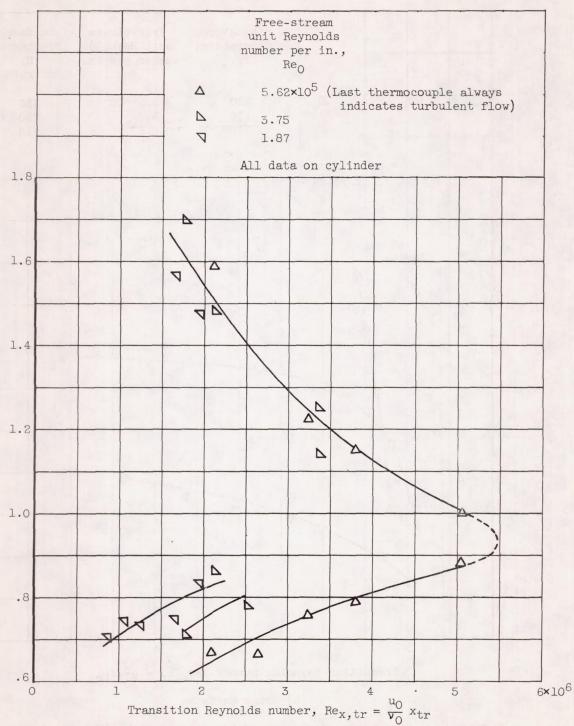 number for hemisphere-cone-cylinder.

4479

Figure 11. - Variation of transition reversal with unit Reynolds number for 120°-cone-cylinder. Surface finish, <4 microinches; stagnation temperature, 530° R.